034432 水利部信息所

TRANSACTIONS OF THE ASAE

GENERAL EDITION
JANUARY/FEBRUARY
VOL. 45 NO. 1

SELECTED CONTRIBUTIONS IN
ENGINEERING FOR AGRICULTURE, FOOD,
AND OTHER BIORESOURCE INDUSTRIES

GENERAL EDITION

Volume 45

Number 1

January/February 2002

TRANSACTIONS OF THE ASAE

This issue is available electronically
in the online ASAE Technical Library.
ASAE members and those affilated with institutions
purchasing a site license can access the full text at
www.asae.org.

Division Editor: ***Thomas R. Way,*** USDA–ARS, Auburn, Alabama

Associate Editors: ***Robert D. Fox,*** USDA–ARS, Wooster, Ohio; ***Robert Grisso,*** University of Nebraska, Lincoln; ***Timothy M. Harrigan,*** Michigan State University, East Lansing; ***W. Clint Hoffmann,*** USDA–ARS, College Station, Texas; ***S. Ed Hughs,*** USDA–ARS, Mesilla Park, New Mexico; ***Neil McLaughlin,*** Agriculture Canada, Ottawa, Ontario; ***Richard L. Parish,*** Louisiana State University, Hammond; ***Graeme R. Quick,*** Iowa State University, Ames; ***Randy L. Raper,*** USDA–ARS, Auburn, Alabama; ***Ronald T. Schuler,*** University of Wisconsin, Madison; ***Kevin J. Shinners,*** University of Wisconsin, Madison; ***Kenneth A. Sudduth,*** USDA–ARS, Columbia, Missouri; ***Randy K. Taylor,*** Kansas State University, Manhattan; ***Harold W. Thistle,*** USDA–FS, Morgantown, West Virginia; ***J. Alex Thomasson,*** Mississippi State University, Mississippi State; ***Shrini Upadhyaya,*** University of California, Davis; ***Jon H. Van Gerpen,*** Iowa State University, Ames; ***Joel T. Walker,*** Ohio State University, Columbus.

此为试读,需要完整PDF请访问: www.ertongbook.com

Design and Evaluation of a Low–Power Portable Test Rig for Vibration Tests on Mobile Agricultural Machinery

J. Anthonis, K. Deprez, H. Ramon

Abstract. *Increased capacity of mobile agricultural machinery and higher driver comfort requirements force manufacturers to incorporate dynamic behavior explicitly into the design. Therefore, vibration tests should be carried out during the design phase. Because many of these manufacturers are small, they lack the know–how and equipment to perform these tests. Transportation to and from specialized companies to evaluate the vibrational characteristics is costly and time–consuming because of the size and weight of most agricultural machinery. A low–power mobile electro–hydraulic shaker allows such analysis to be performed on the factory floor. Such a device can be created by putting an air spring parallel to the actuator of an electro–hydraulic shaker, resulting in considerable power savings. A shaker with and without a parallel spring is theoretically examined. Experiments on a one–degree–of–freedom vertical shaker showed good agreement with the theory and demonstrated that different mode shapes of an agricultural tractor can be sufficiently excited with a nominal hydraulic power of 500 W.*

Keywords. *Electro–hydraulic shaker, Low power, Resonance frequencies.*

The growing importance of and interest in vibrations of mobile agricultural machinery, forestry machinery, and other off–road vehicles force machine manufacturers to incorporate dynamics into their basically static designs. Vibrations are induced by soil unevenness, moving elements within the machine, or implements. Due to high vehicle speeds and increased capacity pushed by labor costs, large–scale production, and a competitive environment, vibration levels have also increased. Neglecting machine dynamics in the design results in reduced or poor performance, operator discomfort, health problems, and increased noise.

Poor performance due to ignoring dynamic phenomena is found in agricultural sprayers where a 40 m working width of the spray boom is noted. Proper application of agro–chemicals is achieved by a constant height and a uniform speed of the spray boom across the field. Modern spray booms are lightweight, flexible structures that exhibit large motions during field operation, resulting in an unacceptable spray deposit distribution (Ramon and De Baerdemaeker, 1997; Ramon et al., 1997).

Vibration levels between 0.5 and 20 Hz may also affect the health of the operator, who may experience low back pain after some hours of operation, resulting in long–term severe physical damage (Magnusson et al., 1996). Research pointed out that low back pain is the leading cause of industrial disability for workers younger than 45 years of age (Pope and Hansson, 1992). Measurements on tractor drivers showed abnormal radiographic changes of the spine in 61% of the cases of drivers with more than 700 tractor driving hours per year. For more than 1200 driving hours per year, abnormal radiographic changes of the spine are detected in 94% of the cases (Christ and Dupuis, 1966). Similar results have been reported for drivers of heavy earth–moving equipment and truck drivers (Boshuizen et al., 1992; Pope and Hansson, 1992). As a consequence, several national, European, and international standards appeared in order to evaluate the vibration exposure to individuals (EN 1032, EN 30326–1, ISO 2631/1, ISO 5007, ISO 5008, ISO 10326–1, prEN 1031).

From the previous discussion, it is clear that manufacturers show a growing interest in the dynamic behavior of mobile off–road machinery on the one hand, while they are forced, on the other hand, by the client's needs to conform with national and international standards. Therefore, machinery manufacturers need equipment to evaluate vibration levels on their machines. Unfortunately, many manufacturers in agriculture and forestry are small companies that cannot afford the high investment of a large shaker. In addition, most of these companies lack the know–how and the experience to carry out specialized tests to measure vibrations, let alone to evaluate them. Therefore, consulting companies having vibration specialists should be involved in the design process. Transportation of mobile agricultural machinery to these companies can be time–consuming and costly. Furthermore, the number of agricultural machinery produced is often small, and the manufacturing company may not be able to afford to leave their machine at the vibration test company for several weeks. If consulting companies specializing in

Article was submitted for review in October 1999; approved for publication by the Power & Machinery Division of ASAE in November 2001.

The authors are **Jan Anthonis**, Research Engineer, **Koen Deprez**, Research Engineer, and **Herman Ramon**, Department of Agro–Engineering and Economics, Laboratory for Agro–Machinery and Processing, Leuven, Belgium. **Corresponding author**: Jan Anthonis, Laboratory of Agricultural Machinery and Processing, Department of Agro–Engineering and Economics, K.U. Leuven, Kardinaal Mercierlaan 92, 3001 Heverlee, Belgium; phone: +32 (0) 16 32 7678; fax: +32 (0) 76 32 7996; e–mail: jan.anthonis@agr.kuleuven.ac.be.

© 2002 American Society of Agricultural Engineers ISSN 0001–2351

vibration analysis can create a small and inexpensive mobile test rig, then tests could be performed on the factory floor without requiring major investment by the machine manufacturer. Tests *in situ* have the additional advantage that quick adaptations to the tested structure can be made by the manufacturer.

Objectives

A low–power, one–degree–of–freedom, mobile, vertical shaker was designed that enabled evaluation of the vibration characteristics of agricultural machinery. A spring parallel to the hydraulic actuator compensates for gravity and allows for a considerable amount of power reduction.

The dynamic behavior of a shaker, with and without a parallel spring, was investigated theoretically by deriving the equations of motion. Based on insights from these equations, design choices were made to obtain a mobile shaker requiring only a small amount of power to perform vibration tests.

After the construction of the shaker, experiments on a tractor proved that with a small amount of power, the dynamic behavior of vehicles can be analyzed. In addition, some special phenomena encountered during the theoretical study were experimentally confirmed.

Theoretical Study of Shakers With and Without a Parallel Spring

Within the framework of the SPECS Project (1994–1998), it was proven that an agricultural tractor could be considered as a linear system. This implies that the superposition principle is valid, such that modal models built with input excitations alternately under one of the wheels can be combined. Excitation directly under the tires is possible because most off–road machinery lacks any type of suspension, contrary to cars and trucks, to avoid disturbing performance during off–road operation. Modal analysis on a lawn mower (Clijmans et al., 1996) and on an agricultural tractor (Clijmans et al., 1998) confirmed these findings and showed that all important modes of the tractor are controllable from the contact area of any tire with the soil. Therefore, a simple one–degree–of–freedom shaker will suffice to evaluate the vibration levels on agricultural machinery.

The force required to excite a vehicle is derived for a shaker without a parallel spring and afterwards extended for a shaker with a parallel spring. Subsequently, power computations are performed. The derivations are based on the theory of vibrations, for which a considerable number of standard works exist in literature (Shabana, 1997; Inman, 1996; Weaver et al., 1990).

Figure 1 shows a one–degree–of–freedom shaker with a vehicle. Only the first mode of the vehicle is displayed by the mass–spring–damper system with mass (m), spring stiffness (k_1) and the damping constant (c_1). The total displacement (i.e., static and dynamic displacement) of the vehicle and the platform are called x_1^t and x_2^t, respectively. These variables, x_1^t and x_2^t, are split into a static part (superscript 0) and a dynamic part (no extra superscript):

$$x_1^t = x_1 + x_1^0 \tag{1}$$

$$x_2^t = x_2 + x_2^0 \tag{2}$$

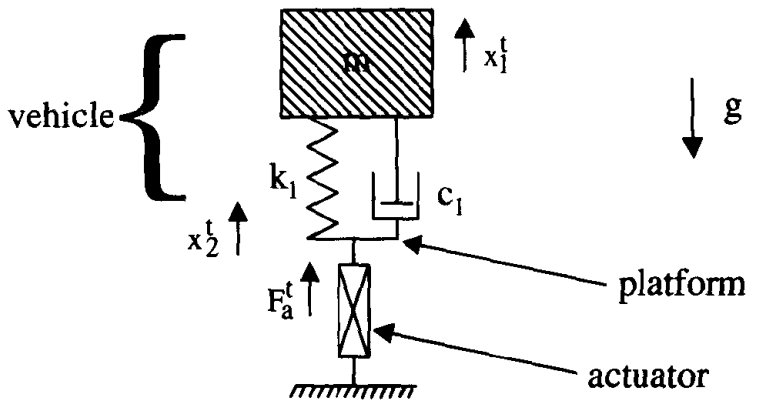

Figure 1. One–degree–of–freedom shaker without parallel spring and loaded with a vehicle.

The positions of the mass (vehicle) or the platform, when there is a vehicle on it and when the system is in equilibrium, are called the static displacements (x_1^0,x_2^0), while the dynamic displacements (x_1, x_2), are the positions of the mass and the platform with respect to the equilibrium state when the system is in motion. The gravitational force acts in the vertical direction and is represented by mg. The objective is to find a relationship between the total actuator force (F_a^t) and the dynamic displacement of the platform (x_2).

When the system is in static equilibrium, the required actuator force (F_a^0) equals the gravity force, and the spring deflection can be written as:

$$F_a^0 = mg \tag{3}$$

$$-k_1(x_1^0 - x_2^0) = mg \tag{4}$$

Writing the equations of motion for the platform and the mass m results in:

$$m\ddot{x}_1^t = -mg - k_1(x_1^t - x_2^t) - c_1(\dot{x}_1^t - \dot{x}_2^t) \tag{5}$$

$$F_a^t + k_1(x_1^t - x_2^t) + c_1(\dot{x}_1^t - \dot{x}_2^t) = 0 \tag{6}$$

Equations 1 and 2 are inserted into equations 5 and 6, simplified by equation 4, and transformed into the Laplace domain, with s as the Laplace operator:

$$(ms^2 + c_1 s + k_1)x_1 = (c_1 s + k_1)x_2 \tag{7}$$

$$F_a^t = -(c_1 s + k_1)x_1 + (c_1 s + k_1)x_2 + mg \tag{8}$$

Eliminating the dynamic displacement of the mass (x_1) from equation 8 by using equation 7 results in the desired relationship between the total actuator force (F_a^t) and the dynamic displacement of the platform (x_2):

$$F_a^t = \frac{(c_1 s + k_1)ms^2}{ms^2 + c_1 s + k_1} x_2 + mg \tag{9}$$

In equation 9, the gravity force must permanently be compensated by the actuator force (F_a^t). This automatically leads to huge actuators, keeping in mind that for an ordinary off–road vehicle the weight per tire is 1.5 to 4 tons. At high frequencies, the total actuator force (F_a^t) increases proportional to the applied frequency. Normally, off–road vehicles

without suspension are solid steel structures with negligible damping ($c_1 \approx 0$), such that at low frequencies, the actuator force is determined by the stiffness (k_1) and the weight (mg) of the vehicle. When the denominator of the first part of the right side of equation 9 approaches zero, the actuator force to be delivered becomes infinity. This frequency occurs at the resonance frequency of the mass–spring–damper system (i.e. the first vertical mode of the vehicle). Harmonic excitation of the vehicle itself at this frequency requires no force. In the field of vibration absorbers, this phenomenon is used to suppress vibrations of machine tools, buildings, and structure–borne noise (Davis and Lesieutre, 2000; Tsai and Lin, 1993). In this case, the vehicle replaces the vibration absorber. If more vertical modes of the vehicle had been incorporated, then these would also be expressed in the denominator of equation 9.

To eliminate the gravity force (mg) in F_a^t in equation 9, a spring is connected parallel to the actuator such that it cancels the gravity force in the neutral static position (fig. 2). The damper (c_2) represents a possible parasitic damping effect in the spring. Collection of the equations describing the neutral static situation gives:

$$F_a^0 = 0 \tag{10}$$

$$-k_2 x_2^0 = mg \tag{11}$$

Equation 4 remains valid.

Again, the objective is to find an expression between the dynamic displacement of the platform (x_2) and the total actuator force (F_a^t). To derive the equations of motion, a reaction force (R) is introduced, as shown in figure 3. The equations of motion of this system are described by equation 3 and the following equations:

$$R + k_1(x_1^t - x_2^t) + c_1(\dot{x}_1^t - \dot{x}_2^t) = 0 \tag{12}$$

$$-R + F_a^t - k_2 x_2^t - c_2 \dot{x}_2^t = 0 \tag{13}$$

Inserting equations 1 and 2 into equations 12 and 13, using equations 4 and 11 and eliminating R, results in:

$$F_a^t + k_1(x_1 - x_2) - k_2 x_2 + c_1(\dot{x}_1 - \dot{x}_2) - c_2 \dot{x}_2 = 0 \tag{14}$$

This equation is transformed into the Laplace domain:

$$F_a^t = [(c_1 + c_2)s + (k_1 + k_2)]x_2 - (c_1 s + k_1)x_1 \tag{15}$$

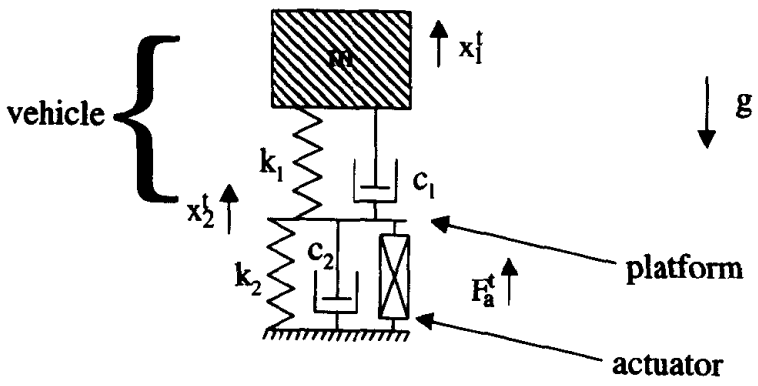

Figure 2. One–degree–of–freedom shaker with parallel spring loaded with a vehicle.

To obtain the desired relation between x_2 and F_a^t, x_1 is eliminated from equation 15 and equation 7:

$$F_a^t = \tag{16}$$

$$\frac{m(c_1 + c_2)s^3 + [m(k_1 + k_2) + c_1 c_2]s^2 + (c_1 k_2 + c_2 k_1)s + k_1 k_2}{ms^2 + c_1 s + k_1} x_2$$

The required actuator force (F_a^t) increases as k_2 and c_2 increase because k_2 and c_2 show up in all terms of the numerator. Therefore, a small parallel spring constant (k_2) and a small damping constant (c_2) are recommended. For a small k_2 and c_2, equation 16 reduces to equation 9 without the additional gravity force.

If the applied displacement spectrum has small band characteristics, then k_2 can be tuned such that the zeros of the numerator coincide with the central frequency of the displacement spectrum to minimize the actuator force. Normally, c_2 is unknown or is a fixed property of the system and cannot be changed. In the case of a conventional shaker, no tuning parameters are available in the numerator of equation 9 because c_1 and k_1 are properties of the vehicle. Consequently, for a shaker without a parallel spring and for a small band displacement spectrum, the required force is higher due to the gravitational force and because there is no tuning parameter to minimize the total actuator force (F_a^t). For an optimized shaker, the parallel spring (k_2) has the function of a temporally energy–storing element.

The required power (P_c) for the conventional shaker and the shaker with a parallel spring (P_s) is obtained by multiplying equations 9 and 16 by the velocity of the platform, or in the Laplace domain by sx_2:

$$P_c = \frac{(c_1 s + k_1)ms^3}{ms^2 + c_1 s + k_1} x_2^2 + mgsx_2 \tag{17}$$

$$P_s = \tag{18}$$

$$\frac{m(c_1 + c_2)s^3 + [m(k_1 + k_2) + c_1 c_2]s^2 + (c_1 k_2 + c_2 k_1)s + k_1 k_2}{ms^2 + c_1 s + k_1} sx_2^2$$

At low frequencies, equations 17 and 18 simplify to:

$$P_c \approx mgsx_2 \tag{19}$$

$$P_s \approx k_2 sx_2^2 \tag{20}$$

From equations 19 and 20, it is clear that at low frequencies only a small amount of power is needed, and the

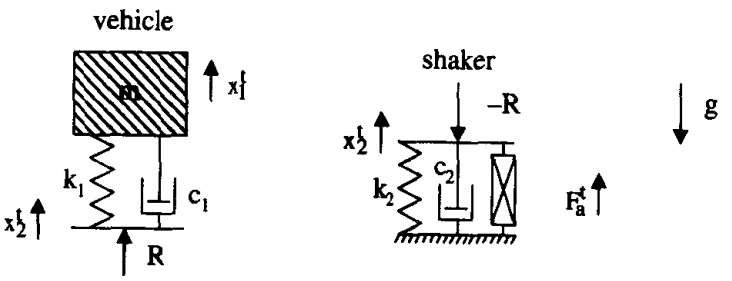

Figure 3. Disconnection of the shaker with parallel spring and the mobile agricultural machine.

power for the shaker with a parallel spring can be made arbitrarily small by decreasing the spring constant (k_2). However, in the case of a conventional shaker without a parallel spring, the actuator must still deliver the gravitational force.

In a higher frequency band, in which ms^2 is larger than k_1, equations 17 and 18 can be further simplified. For many mobile pieces of machinery, c_1 and c_2 are much smaller than k_1 such that for mid–range frequencies, $c_1 s$ is still negligible to k_1, reducing equation 17 to:

$$P_c \approx (k_1 x_2 + mg) s x_2 \tag{21}$$

At the mid–frequency range, where ms^2 is larger than k_1, $m(c_1 + c_2)s^3$ is still considerably smaller than $m(k_1 + k_2)s^2$ such that equation 18 can be approximated by:

$$P_s \approx \frac{m(k_1 + k_2)s^2 + (c_1 k_2 + c_2 k_1)s + k_1 k_2}{ms} x_2^2 \tag{22}$$

Furthermore, due to the suppositions made, $m(k_1 + k_2)$ is the largest term in the numerator of equation 22, which can be reduced to:

$$P_s \approx (k_1 + k_2) s x_2^2 \tag{23}$$

Choosing a small value of k_2, and taking into account that at these frequencies only small displacements (x_2) are applied, which additionally leads to considerable power savings, especially when $k_1 x_2$ has the same or a smaller order of magnitude than mg, it can be concluded that most power is saved when the second term of the right side (STRS) of equation 17 has the same or higher order of magnitude than the first term, and equation 18 has equal or smaller order of magnitude than the first term of the right side (FTRS) of equation 17. For moderate frequencies and small c_2 and k_2, with respect to c_1 and k_1, equation 18 reduces to the FTRS of equation 17, as demonstrated by equations 21 and 23. When narrow–band excitation signals are employed, k_2 can be tuned such that equation 18 becomes smaller than the FTRS of equation 17.

In order to keep the FTRS below the STRS of equation 17, it should be noted that at high frequencies, the amplitude of the displacement input (x_2) should be small, as x_2 appears in the FTRS of equation 17 with a power of 2 and in the STRS with only a power of 1. Furthermore, for weakly damped vehicles, c_1 is small, such that at moderate frequencies $c_1 s$ is negligible to k_1, providing two terms with the same power of s in equation 17. In this way, the FTRS of equation 17 can be kept smaller than the STRS of equation 17. It is most likely that heavy off–road machines are only excited by low– or at most moderate–frequency terrain unevenness (i.e., displacement inputs), which can be explained by the large mass and low travel speed of these vehicles.

Design of a Low–Power Portable Test Rig

The theoretical analysis recommends a parallel spring with a small spring constant (k_2) to save power. However, as this would require a stroke too long, an air spring is employed, which is frequently used in truck suspensions. The characteristics of the selected air spring (1T14F–2 Airstroke actuators and Airmount isolators; Firestone, 1994) are depicted in figure 4. In the range between approximately 160 mm and 280 mm, the curves show an almost flat course, implying a very small spring constant. Unfortunately, the curves are measured with a constant pressure, which can only be guaranteed when the air spring is connected to a compressor or a very large pressure tank. Therefore, the characteristics of the spring were measured in a locked state without connection using a compressor or a very large pressure vessel.

Measurement results are shown in figure 5. The measurements were carried out for six different initial pressures from 1 bar to 6 bar in steps of 1 bar. The initial pressures were applied when the air spring was in its working range of 0.21 m. During the experiments, care was taken to prevent the maximum pressure in the air spring from exceeding 8 bar during compression. As is clear from figure 5, the spring constant (k_2) is much higher when the spring is in a locked state. In addition, the measured curves show hysteresis, which is actually a non–ideal behavior of the spring that can be modeled as damping. For displacement inputs up to

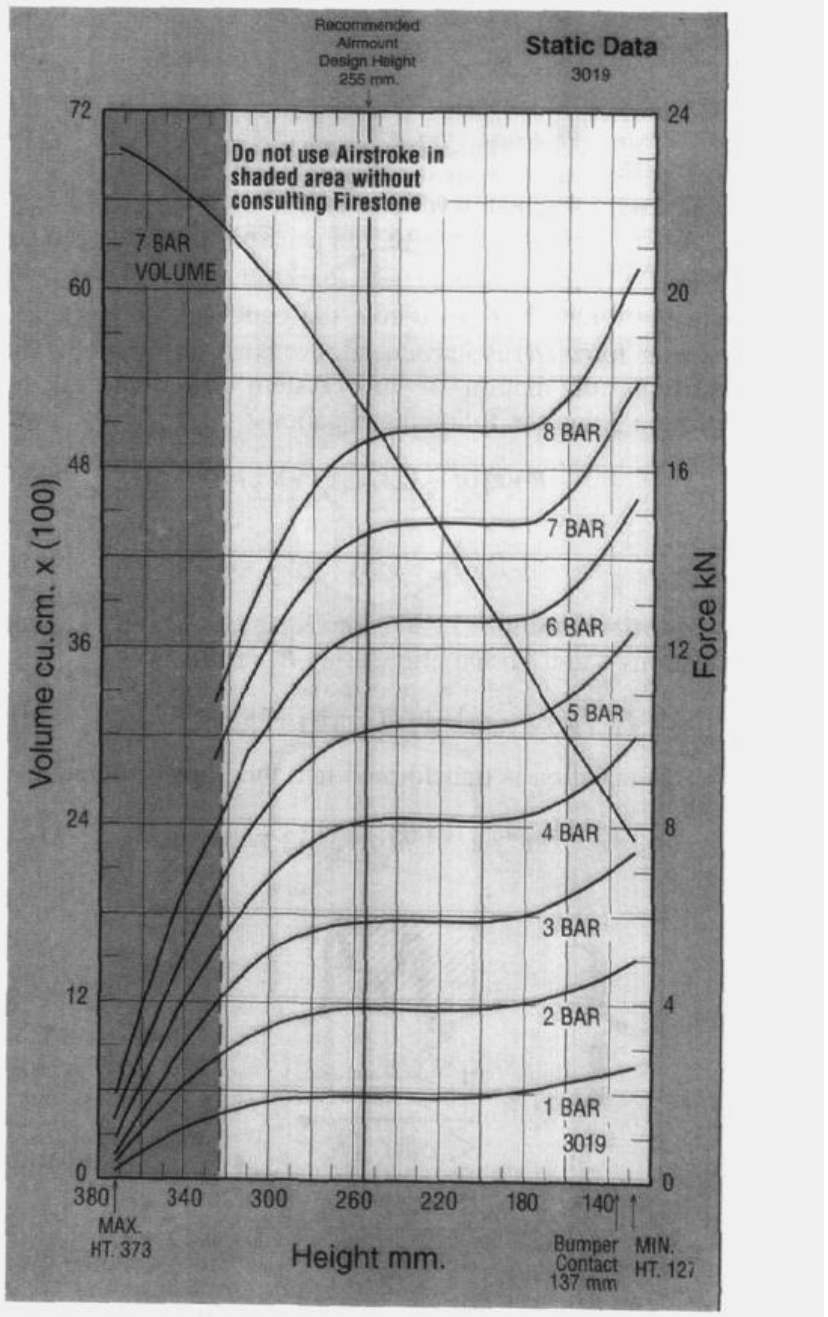

Figure 4. Constant pressure characteristics of an air spring (1T14F–2 Airstroke actuators and Airmount isolators; Firestone, 1994).

0.04 m, which is a common range for modal analysis, almost no hysteresis exists, and the curves can be approximated by a straight line (not shown in fig. 5).

The air spring behavior can be modeled easily. As can be seen from figure 4, the force–displacement curves are almost flat in the working range. Furthermore, by locking the air spring, the force displacement curves obtain a slope. This implies that the behavior of the air spring is almost entirely governed by the behavior of the air inside the spring and not by the rubber material of the spring. During vibration experiments, the spring compresses and decompresses, and the temperature of the air in the spring goes up and down. However, as these temperature changes are relatively rapid, there is no time for the spring to exchange heat with the environment. Therefore, the changes of the state of the air into the spring correspond to the law of adiabatic compression:

$$pV^{\kappa} = \text{constant} \tag{24}$$

where p is the absolute pressure of the air in the spring, V is the volume of the spring, and κ is the constant of adiabatic compression, which is 1.4 for air. In hydraulics, the behavior of accumulators is also modeled by equation 24 (Findeisen and Findeisen, 1994).

Spring stiffness (k_s) is defined as the change in spring force (F_s) due to an incremental change in spring length (l_s) or:

$$k_s = \frac{dF_s}{dl_s} \tag{25}$$

Therefore, the spring stiffness can be calculated by equation 25 by differentiating equation 24. Replacing p by F_s/A_s and V by $A_s l_s$, where A_s is the cross–section of the air spring, renders the spring stiffness:

$$k_s = \frac{dF_s}{dl_s} = \frac{\kappa . p . A_s^2}{V} \tag{26}$$

There is no negative sign in equation 26 when F_s is considered as the force exerted on the spring. Note that for the derivation of equation 26, changes of the cross–section (A_s) during compression and expansion are neglected. In a certain working range, equation 26 may be considered as constant. To verify the validity of equation 26, a mass (m_s) is put on the air spring, and the eigenfrequency (f_e) is measured and calculated:

$$f_e = \frac{1}{2\pi}\sqrt{\frac{k_s}{m_s}} \tag{27}$$

Pumping the air spring to 0.23 m height with a mass (m_s) of 193 kg results in an absolute pressure of 2 bar. The spring area (A_s) is taken from the manufacturer's data and amounts to 196×10^{-4} m^2. Calculation of equation 26 renders an eigenfrequency of 1.77 Hz. The eigenfrequency is measured by putting the air spring with mass (m_s) on a shaker and applying a sweptsine or shirp (i.e., a sine wave with linear increasing frequency) or:

$$\sin[(at + b)t] \tag{28}$$

where a and b are constants. Figure 6 shows the measured frequency response function. An eigenfrequency of 1.85 Hz can be observed, corresponding to the measurements. As can be seen from equation 26, the spring stiffness and the eigenfrequency (eq. 27) can be lowered by increasing the volume (V) of the air spring, which can be achieved by attaching a barrel to the air spring. A barrel of 12 L was connected to the air spring, which produced a predicted eigenfrequency of 0.92 Hz. Figure 7 shows the measurements, indicating an eigenfrequency of 1 Hz. Due to damping introduced by the connection between the air spring and barrel, the resonance peak is reduced considerably comparing to figure 6.

For practical reasons, the air spring, mounted in the shaker, is kept in a locked state, although this is less favorable than using it at constant pressure or by attaching a barrel to it. Compared to a mechanical spring, it has the additional advantage that no adjustments have to be made to keep the shaker in neutral position when a vehicle with a different weight is placed on the shaker. It is just a matter of inflating the air spring until the shaker reaches its neutral position, here at 0.21 m. After this operation, experiments can start immediately.

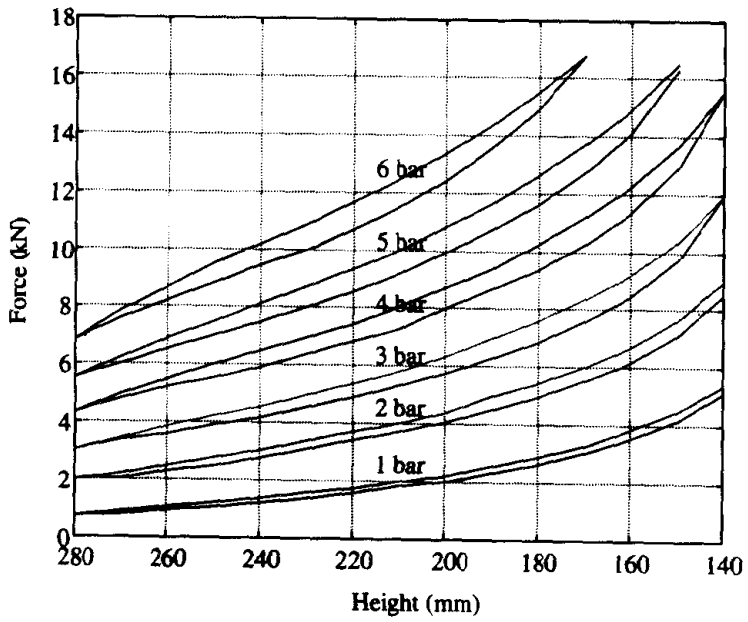

Figure 5. Characteristics of a locked air spring (1T14F–2 Airstroke actuators and Airmount isolators; Firestone, 1994).

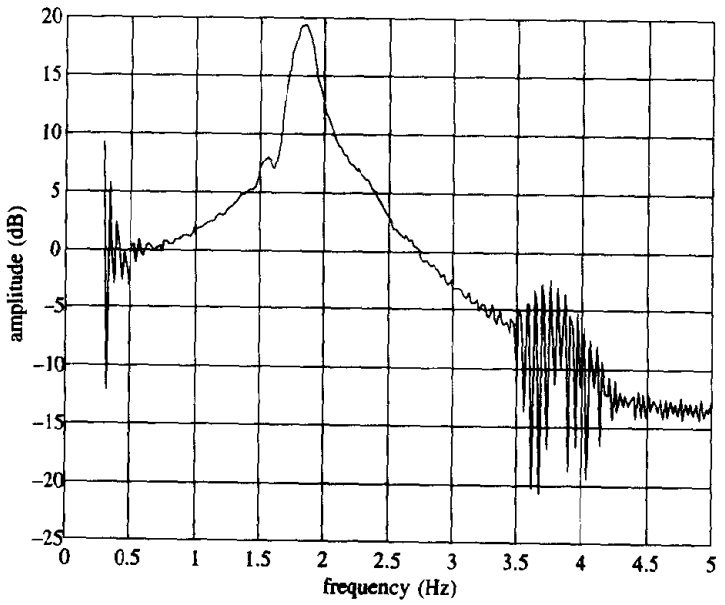

Figure 6. Measured frequency response function (FRF) of the air spring with a mass of 193 kg.

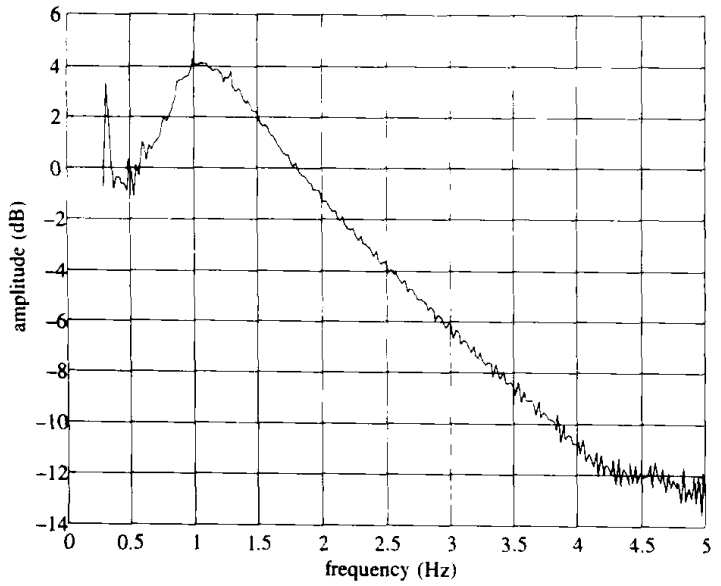

Figure 7. Measured frequency response function (FRF) of the air spring connected to a barrel of 26 L with a mass of 193 kg on the air spring.

Figure 8 shows a sketch of the shaker, which is placed under one wheel of the vehicle. Owing to the revolute joint, the platform on which the vehicle is placed performs a circular motion. However, as the wheel of the vehicle is placed above the air spring, which is approximately 2 m from the axis of rotation, and taking into account the actuator displacement, which is in the range of 0.05 m, the motion of the wheel of the vehicle is quasi–vertical.

The actuator is a hydraulic, double–acting, double–rod linear cylinder having a stroke of 0.1 m, a net area of 2.9×10^{-4} m^2 (Rexroth, type CG 70 E 25/16–XXZ13/01 HFUM11T), and equipped with a four–way servovalve (Rexroth, type 4 WS 2 EM6–1 X/5B1ET315Z7EM) of the critical center type with a nominal flow rate of 3 L/min at a pressure drop of 70 bar over the valve. The supply pressure from the hydraulic group is tuned on 100 bar.

The hydraulic cylinder is position controlled by an analog PID controller (Rexroth Servoverstärker VT 1600 S3X). Positions are measured by means of an LVDT type sensor (Solartron DC 50).

EXPERIMENTS

Experiments were carried out on an agricultural tractor (International 845 4–WD) supplied with a front ballast of 300 kg. The shaker depicted in figure 8 was put under the left rear wheel of the tractor, while the other wheels were placed on platforms having the same height as the shaker (i.e., 0.5 m). The tractor is harmonically excited under its left rear tire by 61 single sine waves starting at 0.1 Hz and increasing in frequency up to 21 Hz. These excitation signals are generated by a PC and forwarded by a plug–in D/A board to the PID controller of the actuator. The position of the platform of the shaker is measured through an LVDT sensor and recorded by an A/D board on the PC. During the experiments, the reference amplitude was kept at 0.011 m. For each excitation, the amplitude of the shaker was measured through the LVDT sensor, and the most important resonance frequencies and their corresponding mode shapes were recorded (table 1).

Measurement of the resonance frequencies and mode shapes has been performed in a manner similar to Clijmans et al. (1998). Explanations of the mode shapes roll, pitch, yaw, and jump are shown in figure 9. The measured vertical amplitude versus frequency is shown in figure 10. At resonance frequencies with vertical components (i.e., pitch, roll, jump, and eventually the cab resonance), dips are observed in the graph. This is completely in agreement with equation 16, where the resonance frequencies of the mode shapes with vertical components of the excited vehicle appear in the denominator of the expression, resulting in large actuator forces. Because it is physically impossible to exceed the maximum deliverable actuator force, the amplitude of the excitation is decreased. Yawing has no vertical component in its mode shape; consequently, no dip is visible in the graph at this resonance frequency.

It should be noted that although the amplitude of the excitation is very low at the resonance frequencies of the mode shapes with vertical components, the vibration level of the vehicle is very high. During the experiments, other resonance frequencies than the ones listed in table 1 were noted (e.g., resonances of the motor hood and the exhaust pipe), but they are not relevant to the discussion here. From the experiment, it may be concluded that the shaker is able to excite the eigenfrequencies of the tractor, and a good agreement between theory and practice is found.

Concerning force and power computations, given the net cylinder area of 2.9×10^{-4} m^2 and the operating pressure of

Table 1. Resonance frequencies of the tractor and corresponding mode shapes.

Mode Shape	Resonance Frequency (Hz)
Pitch	1.3
Roll	1.8
Jump	3.4
Yaw	4.4
Cab resonance	9.5

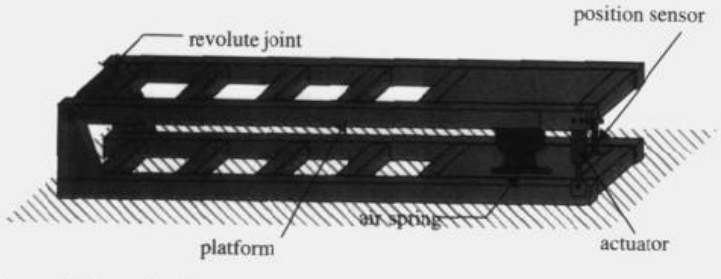

Figure 8. Sketch of the portable, low power, one–degree–of–freedom test rig.

Figure 9. Explanation of the mode shapes roll, pitch, yaw, and jump.

此为试读,需要完整PDF请访问: www.ertongbook.com

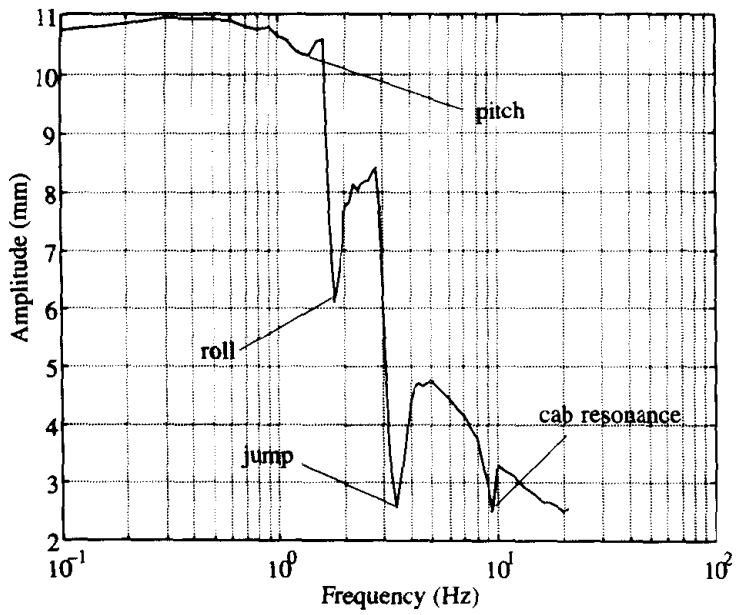

Figure 10. Measured achieved vertical position of the shaker as a function of frequency (desired 0.011 m).

100 bar, a simple calculation renders a maximum applicable force of the cylinder of 2900 N and a nominal hydraulic power of 500 W. The air spring, used in a locked state around its equilibrium position of 0.21 m and not at constant pressure, requires a force of about 800 N when an amplitude of 0.01 m is desired (fig. 5). At high frequencies, the achieved amplitudes of the shaker are smaller, such that not much is gained by operating the air spring at constant pressure.

If no parallel spring had been used, then the cylinder would not have been able to lift the tractor tire, keeping in mind a weight of approximately 11000 N under one rear tire. For a shaker configuration without a parallel spring that has to reach the same performance as the tested one, a supplementary force around 2000 N must be taken into account to excite the tractor. This results in a net area of the cylinder of 13×10^{-4} m^2 at a constant operating pressure of 100 bar. To achieve the same cylinder speed, valves with a nominal flow rate of at least 13.5 L/min would be required, resulting in a hydraulic power of 2250 W, which is a 4.5 times higher power consumption.

Although the presented shaker with a parallel spring is well suited to experimentally determine the dynamic behavior of vehicles, it is not appropriate to perform fatigue tests. In such cases, large amplitudes, demanding a huge amount of power, are required, such that the contribution of the weight in the power calculation becomes negligible.

As described previously, no optimization was performed for narrow–band excitations with respect to the stiffness of the parallel spring in order to minimize the required actuator force and the power of the hydraulic equipment. In case of the air spring, this can be attained by connecting the air spring to a pressure vessel, the volume of which can be varied. In this way, the slope of the force displacement curves is varied, as can be understood by comparing figure 4 and figure 5. Of course, the shaker will become more sophisticated, and the amount of saved power compared to the extra construction cost can be questioned.

Conclusions

A low–power portable test rig was designed. A spring parallel to the actuator of the shaker reduces the power requirements considerably. By restricting power and by limiting the shaker to one vertical degree of freedom, the test rig can be made small and easy to transport. Despite its small size, the low–power, one–degree–of–freedom vertical test rig was able to excite the modes of a heavy agricultural tractor.

Theoretical analysis showed that at the vertical modes of the vehicle, the motions applied by the shaker were limited to very small amplitudes due to high force requirements, but they are well visible by the nature of the mode itself. Experiments confirmed these findings in practice.

Supplementary power can be saved by operating the air spring at constant pressure, which can be realized by connecting the air spring to a large vessel. For narrow–band excitation signals, the input force can be minimized by adjusting the spring stiffness of the shaker, resulting in extra power savings. However, these operations lead to a more sophisticated shaker.

The presented shaker is well suited for evaluating the dynamic behavior of heavy vehicles (e.g., by an experimental modal analysis), but it is not appropriate for fatigue tests where large amplitudes are required, such that the benefit of compensating for the gravitational force in the hydraulic power vanishes.

Acknowledgements

This work was partially supported by Craft Project FA–S2–9009.

References

Boshuizen, H. C., P. M. Bongers, and C. T. J. Hulshof. 1992. Self–reported back pain in fork lift truck and freight container tractor drivers exposed to whole–body vibration. *Spine* 17(1): 59–65.

Christ, W., and H. Dupuis. 1996. Über die Beanspruchung de Wirbelsäule unter dem Einfluss sinusförmiger und stochastischer Schwingungen. *Int. Z. Angew. Physiol. Arbeitsphysiol.* 22: 258.

Clijmans, L., H. Ramon, J. Langenakens, and J. De Baerdemaeker. 1996. The influence of tyres on the dynamic behaviour of a lawn mower. *J. Terramechanics* 33(4): 195–208.

Clijmans, L., H. Ramon, and J. De Baerdemaeker. 1998. Structural modification effects on the dynamic behavior of an agricultural tractor. *Trans. ASAE* 41(1): 5–10.

Davis, C. L., and G. A. Lesieutre. 2000. An actively tuned solid–state vibration absorber using capacitive shunting of piezoelectric stiffness. *J. Sound and Vibration* 232(3): 601–617.

EN 1032. 1996. (E) Mechanical vibration: Testing of mobile machinery in order to determine the whole–body vibration emission value: General requirements. European standard.

EN 30326–1. 1994. (E) Mechanical vibration: Laboratory method for evaluating vehicle seat vibration. Part 1: Basic requirements (ISO 10326–1: 1992). European standard.

Findeisen, D., and F. Findeisen. 1994. *Ölhydraulik: Handbuch für die hydrostatisch Leistungsübertragung in der Fluidtechniek* 4. Heidelberg, Germany: Springer–Verlag.

Firestone. 1994. Airstroke® actuators and Airmount® isolators. Carmel, Ind.: Firestone Industrial Products Company.

Inman, D. J. 1996. *Engineering Vibration.* Englewood Cliff, N.J.: Prentice Hall International, Inc.

ISO 2631/1. 1985. (E) Estimation of the exposure of whole–body vibrations on individuals. Part 1: General specifications. International standard.

ISO 5007. 1990. (E) Agricultural wheeled tractors, operator's seat: Laboratory measurement of transmitted vibration. International standard.

ISO 5008. 1979. (E) Agricultural wheeled tractors: Measurement of vibrations transmitted globally to the operator. International standard.

ISO 10326–1. 1992. (E) Mechanical vibration: Laboratory method for evaluating vehicle seat vibration. Part 1: Basic requirements. International standard.

Magnusson, M. L., M. H. Pope, D. G. Wilder, and B. Areskoug. 1996. Are occupational drivers at increased risk for developing musculoskeletal disorders? *Spine* 21(6): 710–717.

Pope, M. H., and T. H. Hansson. 1992. Vibration of the spine and low back pain. *Clinical Orthopaedics and Related Research* 279: 49–59.

prEN 1031. 1993. (E) Measurement and evaluation of whole–body vibration: General requirements.

Ramon, H., and J. De Baerdemaeker. 1997. Spray boom motions and spray distribution: Part 1. Derivation of a mathematical relation. *J. Agric. Eng. Research* 66(1): 23–29.

Ramon, H., B. Missotten, and J. De Baerdemaeker. 1997. Spray boom motions and spray distribution: Part 2. Experimental validation of the mathematical relation and simulation results. *J. Agric. Eng. Research* 66(1): 31–39.

Shabana, A. A. 1997. *Vibration of Discrete and Continuous Systems.* 2nd ed. New York, N.Y.: Springer–Verlag.

SPECS Project. 1994–1998. SPECS Project Final Report (1 Nov. 1994 to 30 Apr. 1998). Heverlee, Belgium: Laboratory of Agro–Machinery and Processing.

Tsai, H.–C., and G.–C. Lin. 1993. Optimum tuned–mass dampers for minimizing steady–state response of support–excited and damped systems. *Earthquake Engineering and Structural Dynamics* 22(11): 957–973.

Weaver, W., S. P. Timoshenko, and D. H. Young. 1990. *Vibration Problems in Engineering.* 5th ed. New York, N.Y.: John Wiley and Sons.

Development of a Seedling Pick-Up Device for Vegetable Transplanters

W. C. Choi, D. C. Kim, I. H. Ryu, K. U. Kim

Abstract. *A new seedling pick–up device for vegetable transplanters was developed and evaluated in a laboratory. The pick–up device extracts seedlings from a 200–cell tray and transfers them to a position from which they can be transplanted into the soil. The device consists of a path generator, pick–up pins, and a pin driver. The path generator is a five–bar mechanism comprised of a fixed slot, a driving link, a driven link, a connecting link, and a slider. The slider is constrained to move along the driven link and a fixed slot of combined straight–line and circular paths. The connecting link joins the driving link and the slider. When the slider moves along the straight–line path of the slot, it takes a seedling from a cell. When it moves along the circular path, it transfers the seedling to the transplanting hopper. The slider is an assemblage of pick–up pins and a pin driver, which are integral parts of the device. Operational parameters such as seedling age, approach direction of the pins, penetration depth of the pins into the cell, seedling holding method, and extracting velocity were examined using a prototype. The device extracted 30 seedlings per minute with a success ratio of 97% using 23–day–old seedlings.*

Keywords. *Vegetable transplanter, Seedling pick–up device.*

One of the key components of vegetable transplanters is the seedling pick–up device. This device extracts seedlings from the tray cells and transfers them to the transplanting device, which places them into the soil. Seedling trays are often made of plastic and are slightly flexible so that they can be rolled around the feeding drum as the seedlings are picked up.

Yanmar Agricultural Equipment Co. and Kubota Cooperation, leading agricultural machinery manufacturers in Japan, have developed two of the most common seedling pick–up devices for the vegetable transplanters widely used in Korea and Japan. The Yanmar–type moves the pick–up pins toward the lower part of the cell surface and extracts the seedling from the cell while moving along a path in an open, counter–clockwise loop. The Kubota–type generates a crossed path when picking up seedlings by using a more sophisticated mechanism comprised of a slider, cam, and links. Although these two pick–up devices perform well, their structural complexity have made them difficult to use for various types of vegetable transplanters. In addition, these pick–up devices are not economically feasible for locally made vegetable transplanters because of their high manufacturing costs (Choi, 2000).

As demand for the mechanization of vegetable production in Korea has increased, many attempts have been made to develop a seedling pick–up device that is structurally simple, functionally accurate, and economically feasible for many locally made vegetable transplanters. This study was one of these attempts. The articles authored by Brewer (1994) and Hassan and Haddock (1991) were reviewed to develop a conceptual framework of a seedling pick–up device that will satisfy such requirements. No other useful literature was available. The objectives of this study were to develop a seedling pick–up device for vegetable transplanters suitable to Korean conditions and evaluate its work performance in a laboratory.

Design Conditions

The design conditions for the seedling pick–up device and the vegetable transplanter to be developed were as follows:

1. Seedling type: plugged seedlings grown in a cell tray.
2. Variety of vegetable: Chinese cabbage.
3. Cell tray: 20 × 10 cells.
4. Cell dimensions: 23 × 23 mm top, 9.5 × 9.5 mm bottom, and 44 mm depth.
5. Transplanting speed: 0.15 to 0.2 m/sec.
6. Planting distance: 30 to 40 cm.
7. Work capacity: 1800 to 2400 plants/hr/row.

These conditions were established on the basis of cultural practice for vegetable production in Korea. Although the working speed seems about the speed of hand placement, it was intended at the beginning of the study to concentrate our

Article was submitted for review in October 2000; approved for publication by the Power & Machinery Division of ASAE in March 2001.

The authors are **Won C. Choi**, Graduate Student, **Dae C. Kim**, Graduate Student, **Il H. Ryu**, Post–Doctoral Fellow, and **Kyeong U. Kim**, ***ASAE Member Engineer***, Professor, Seoul National University, Suwon, Korea. **Corresponding author:** Kyeong Uk Kim, School of Bio–resources and Material Engineering, College of Agricultural and Life Sciences SNU 441–744, Suwon, Korea; phone: 82–31–290–2382; fax: 82–31–297–7478; e–mail: kukim@plaza.snu.ac.kr.

© 2002 American Society of Agricultural Engineers ISSN 0001–2351

efforts on making the function of the seedling pick–up device more accurate.

Development of Seedling Pick-Up Mechanism

Path Generator

The seedling pick–up device consists of three major components: a path generator, pick–up pins, and a pin driver. The path generator generates an appropriate path of approach and regress along which the pick–up pins move for a cycle of work. The pick–up pins extract seedlings from the cells and transfer them to the place where they are to be transplanted into the ground. The pin driver activates the pins to hold seedlings at the cell and then release them at the discharge point. The path of the pick–up pins is the most important factor in the design of a seedling pick–up device and determines the device's performance. When the pins approach a seedling, their direction should be normal to the cell surface for maximum extracting performance. At the discharge point, the pins must be a little upward relative to the vertical to account for the inertia acting on the seedling.

To obtain the best performance of the pick–up device, the path generator needs to satisfy the following requirements:

1. When the pick–up pins penetrate into the root soil of a cell, the penetration depth should be more than 40 mm in a straight line so that the pins can hold the seedling as firmly as possible.
2. The pins should release seedlings at an angle of 75° downward from the horizontal to account for the inertia of the seedlings.
3. The mechanism of the path generator should be simple and easy to manufacture.

A mechanism for the path generator was realized through an evolution of designs. The final design was a five–bar mechanism comprised of a fixed slot, a driving link, a driven link, a slider, and a connecting link joining the slider and driving link. The slider is constrained to move on the driven link and along the combined straight–line and circular paths of the fixed slot. The straight line satisfies the path requirement for the path generator. The slider was later replaced by an assemblage of a pin driver and pick–up pins of an appropriate length, which is an integral part of the seedling pick–up device. Figure 1 shows a schematic diagram of the path generator mechanism.

As the slider moves outward (from left to right in fig. 1) along the straight–line path, the pins approach a seedling in a cell and penetrate into its root soil, squeezing the soil gradually at the same time. When the slider moves back (to the left in figure 1) along the same straight–line path, the pins extract the seedling from the cell. When the slider reaches the end of the straight–line path, it moves along the circular path, which has its center of rotation at the rotational center of the driven link. At the end of the circular path (i.e., at the end of the slot), the pins discharge the seedling into the transplanting hopper. The slider then returns to the starting point of the straight–line path. This completes a work cycle of extracting, transferring, and discharging a seedling.

Problems associated with this type of slider motion include heat and wear due to friction between the slider and

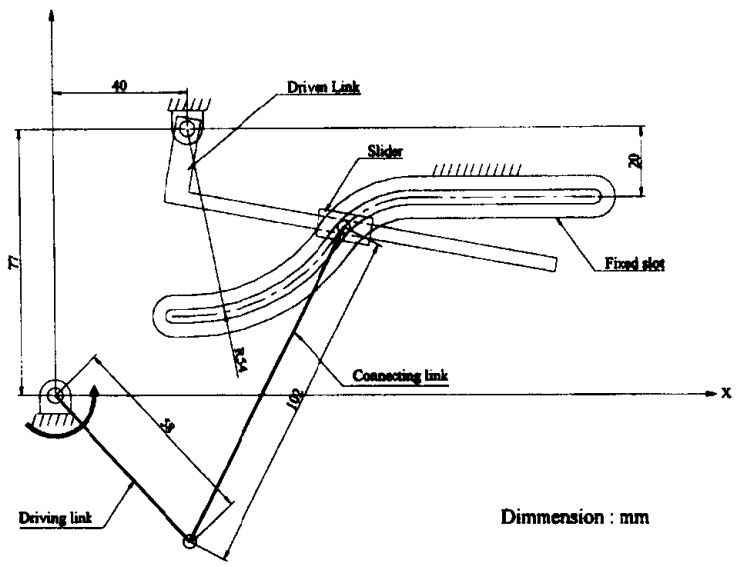

Figure 1. Schematic diagram of the path generator.

slot. These may change the shape and length of the slot, resulting in a loss of accuracy in the extracting and discharging actions of the pick–up pins.

Pin Driver

The pin driver makes the pins squeeze the seedling gradually as they penetrate the cell and then release the seedling when the seedling is discharged. Therefore, the pin driver must be designed to satisfy the following requirements:

1. Extracting and discharging of seedlings should be done precisely at the pre–determined points.
2. Seedlings should be held firmly during the transfer from the extracting to the discharging points.
3. The root soil of seedlings should not be destroyed during extraction and transfer.

After many trials, a pin driver was designed. As shown in figure 2, the pin driver consists of two pick–up pins attached to guide plates and a plunger that reciprocates between the guide plates. The guide plates are pivoted so that the pins are opened as the plunger moves forward and closed as the plunger moves backward. Movement of the plunger is triggered by a spring inside the pin assembly. To remove the seedlings completely from the pins, rings around the pick–up pins are connected to the plunger so that the rings push the seedling out of the pins as the plunger moves forward.

At the start of a work cycle, the plunger moves backward and the pick–up pins close gradually as they approach a seedling in a cell (fig. 2a). At the same time, the pin assembly moves toward the seedling until the pick–up pins hold the soil of the seedling at their maximum penetration depth (fig. 2b). The assembly then moves back to extract the seedling from the cell (fig. 2c). The plunger does not move again until the pin assembly reaches the discharge point. At the discharge point, the plunger moves forward to open the pick–up pins and release the seedlings (fig. 2d).

In order for the pick–up pins to hold seedlings firmly, the inner edges of the guide plates have a 2–mm step, as shown in figure 3. The pins close quickly when the plunger runs over the step. Since the edge line of the guide plates and the diameter of the plunger determine the locus of the pins, these components must be changed for different types of seedlings.

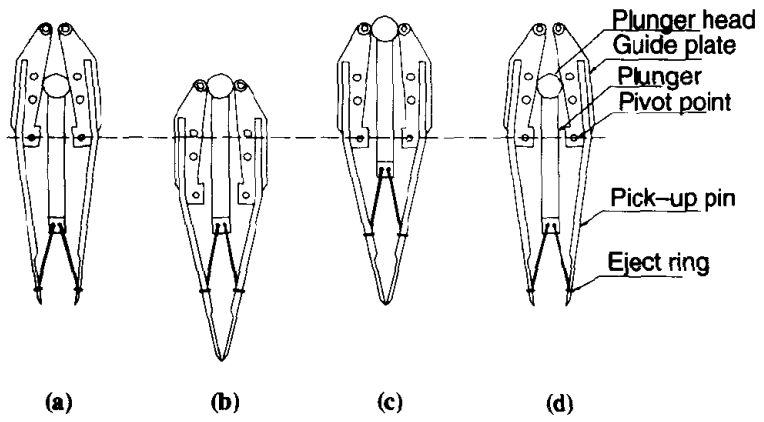

Figure 2. Operation of the pin driver.

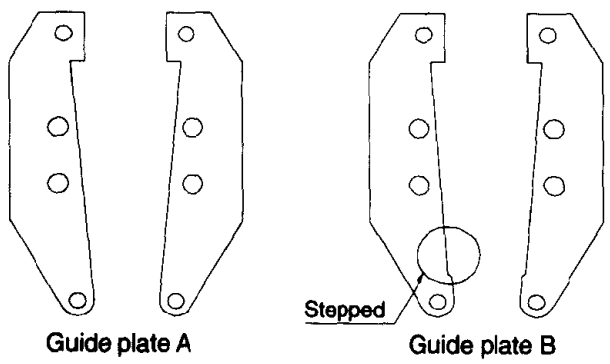

Figure 3. Guide plates.

Pick–Up Pins

The pick–up pins should not break the root soil or drop the seedling during the transfer. In order to avoid soil breakage, the tips of the pins were flattened to a thickness of 1 mm for a length of 20 mm, while the remaining part of the pins was made of rigid round wire 3 mm in diameter, as shown in figure 4.

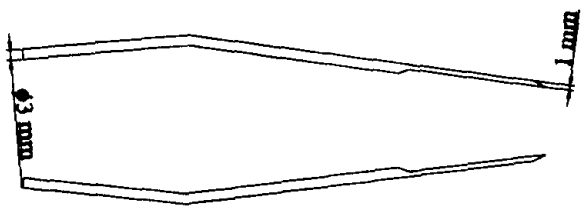

Figure 4. Pick–up pins.

Analysis of Velocity, Acceleration, and Torque

The pick–up device was kinematically modeled using the x–y coordinate system, as shown in figure 1, and its motion was simulated using ADAMS software (Mechanical Dynamics, Inc., Ann Arbor, Mich.) to analyze the velocity and acceleration of the pick–up pins and the input torque required to drive the device. The rotational angle required of the driving link to move the pick–up pins from the extraction point to the discharge point was 189° in the counter–clockwise direction, and the return movement (from discharge point to extraction point) was 171°, so the time ratio of the working to returning phases was 1.1. Figures 5, 6, and 7 show the simulated velocity of the pick–up pins, the simulated acceleration of the pick–up pins, and the input torque required to make a complete revolution of the driving link with a velocity of 30 rpm in the counter–clockwise direction, respectively.

The peak velocity and acceleration were estimated to be 1.4 m/s and 440 m/s^2, respectively, and they were not affected by the rotational direction of the driving link. However, the torque required to drive the device was affected by rotational direction. The peak torque was 2.9 N–m for counter–clockwise rotation, as shown in figure 7, and 4.1 N–m for clockwise rotation. Therefore, the driving link was designed to rotate in the counter–clockwise direction. The mass and inertia data necessary for the torque calculation were created within the ADAMS program when the device was modeled and its material (steel) was specified. When the velocity of the driving link increased from 30 to 40 rpm, seedlings dropped from the pins at the points where peak acceleration occurred. To reduce the peak acceleration at 40 rpm, the rotational center of the driving link was relocated, which reduced the peak acceleration from 757 to 351 m/s^2 without affecting the extracting and discharging of seedlings. The reduced acceleration was about 80% of the peak acceleration at 30 rpm, at which no seedlings were dropped. If the velocity were increased further, then the peak acceleration could not likely be reduced without also affecting the extracting and discharging of seedlings.

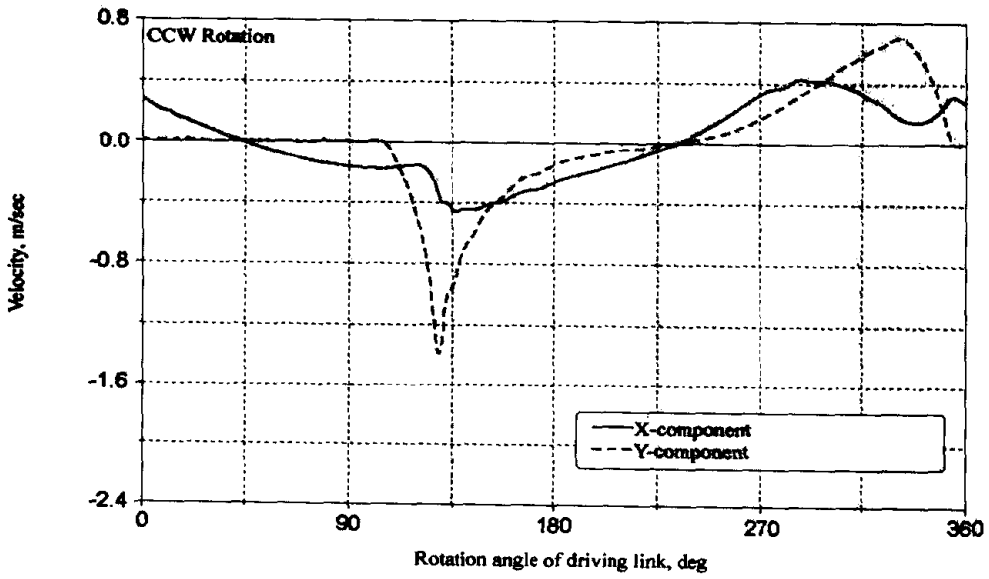

Figure 5. Velocity of pick–up pins.

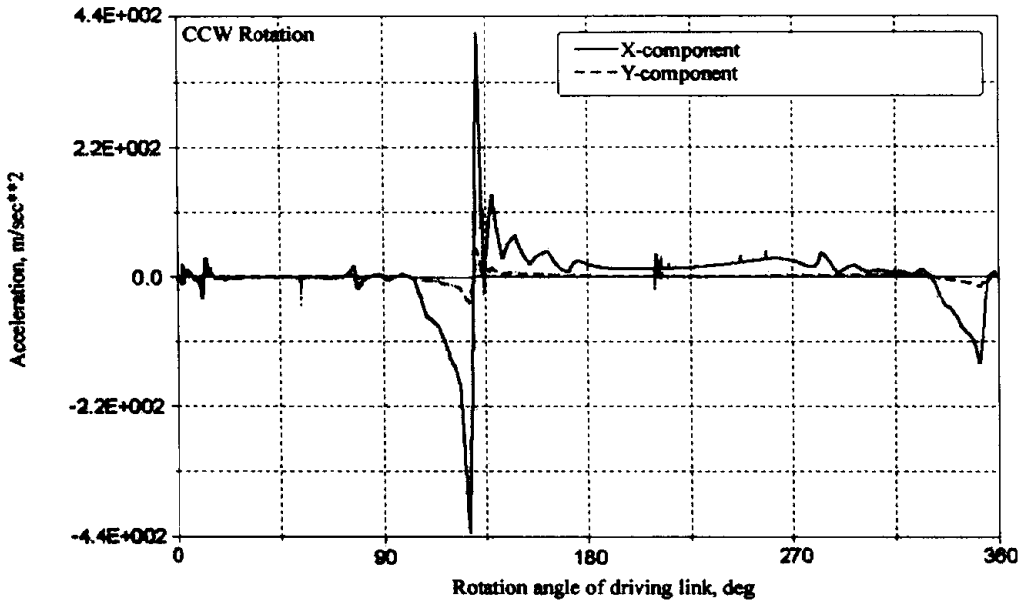

Figure 6. Acceleration of pick–up pins.

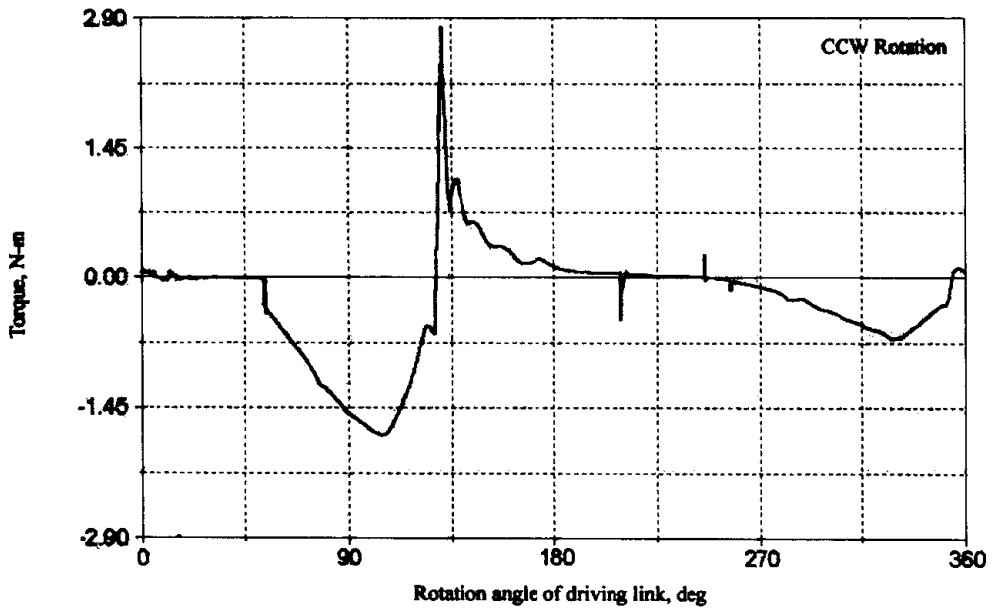

Figure 7. Driving torque.

MODIFICATIONS

A prototype of the seedling pick–up device was constructed and test–operated to examine whether or not its functional requirements were satisfied. The test trials used a plunger with a diameter of 15 mm, and the velocity of the driving link was set to 30 rpm. The following cases were considered functional failures:

1. When the pick–up pins could not extract the seedlings from the cell.
2. When the pick–up pins broke more than 1/4 of the root soil of seedlings.
3. When the pick–up pins tore off leaves of seedlings.

In the first trial, seedlings were not completely ejected from the pins when they were released. This was because the leaves of the seedlings were tangled with the pins, and the movement of the eject rings was not long enough to move the seedlings off the pins.

To prevent the pins from interfering with the frame of the seedling tray, the opening of the pins must be less than the width of a cell. It was found that the optimal opening of the pins was 2 to 3 mm less than the width of cell. To reduce the opening of the pins, the plunger with a diameter of 15 mm was replaced with one of 14 mm, resulting in an opening of 18 mm at the beginning of penetration and 2.5 mm at maximum penetration depth.

When the pins penetrated the root soil to a depth of 41 mm, the final pin depth in the extracted seedlings was found to be about 36 mm due to a pin regress of 5 mm within the root soil. The amount of pin regress increased as pin penetration depth decreased: a penetration depth of 36 mm resulted in a final pin depth of 22 mm. Considering this regress, the pins need to penetrate into the root soil as deeply as possible within the depth of the cell.

In the second trial, guide plates with and without the stepped edges were tested. The guide plates with stepped edges performed better at extraction of seedlings than did those without stepped edges at the same penetration depths. It was also found that the pin ends should be flat for better holding of seedlings within the cell. Using the results obtained from the test trials, the prototype was modified and subjected to a performance test. Figure 8 shows the modified prototype of the seedling pick–up device.

此为试读,需要完整PDF请访问: www.ertongbook.com